

A comparative study of different techniques for microstructural characterization of oil extended thermoplastic elastomer blends

Pratip Sengupta^{a,b}, Jacques W.M. Noordermeer^{a,b,*}

^a Dutch Polymer Institute (DPI), P.O. Box 902, 5600 AX Eindhoven, The Netherlands

^b Department of Rubber Technology, Faculty of Science and Technology, University of Twente, P.O. Box 217, 7500 AE Enschede, The Netherlands

Received 16 June 2005; received in revised form 12 October 2005; accepted 14 October 2005

Available online 11 November 2005

Abstract

This paper gives a relative comparison of different microscopic methods that are presently used to visualize polymer blend morphologies, versus the possibility to visualize the three-dimensional structure of the blends with electron tomography. Oil extended thermoplastic elastomer (TPE) blends based on a high amount of rubber phase and low amount of isotactic polypropylene (PP) were used as samples for this study. Low voltage scanning electron microscopy (LVSEM) and transmission electron microscopy (TEM) proved to be far superior to conventional scanning electron microscopy (SEM) and atomic force microscopy (AFM) for obtaining good quality images of the morphology of these blends. In an attempt to visualize the 3D morphology, electron tomography was carried out on these blends and models of the 3D morphologies were constructed. The usefulness of the different microscopic techniques in providing complementary morphological information and the potential of electron tomography as a new tool for constructing 3D-models of polymer blends are highlighted.

© 2005 Elsevier Ltd. All rights reserved.

Keywords: Thermoplastic elastomers; Electron microscopy; Blends

1. Introduction

Understanding the morphology of polymer blends is important in order to determine relationships between the structure and properties of materials. Microscopic methods like light microscopy (LM), scanning electron microscopy (SEM), low voltage scanning electron microscopy (LVSEM), transmission electron microscopy (TEM) or atomic force microscopy (AFM) can detect details, ranging from the millimetre to the subnanometer scale, and are therefore popular tools for visualising blend morphology: Table 1 [1]. In spite of several spectacular developments in instrumental techniques, structure determination of polymer blends remains a formidable challenge. This is, because most electron microscopic methods are based on observations on thin sections or surfaces that show a cross-section of the three-dimensional structure or only some surface topography that can be influenced by the

sample preparation method. These cross-sections are at best two-dimensional projections of what is a 3D structure, in essence discarding a third of all the spatial information that the specimen may contain. Any specimen variation in the third dimension can be minimised by careful sample preparation, sectioning a specimen in a specific orientation to reveal the features under study and/or by preparing two specimens from mutually perpendicular axes. These approaches work best for specimens with microstructures that are structurally simple, such as a single-phase alloy. For most specimens, however, 2D projections lead to some uncertainty as to their true 3D structure. There are an increasing number of systems whose functions are closely controlled by a complex 3D microstructure. In such cases 2D projections can be at best inadequate, at worst misleading. Because of these reasons, a single 2D microscopic method is not sufficient for unambiguous identification of the blend morphology and in the absence of suitable 3D microstructure visualisation techniques; combinations of several 2D-microscopy techniques are required.

In a blend of two polymers, if the major phase is dispersed in the minor phase, the morphology becomes quite difficult to identify experimentally. Such situations are quite common in soft rubber–thermoplastic blends where the rubber phase is in excess of the plastic phase. If, in addition the blends contain a high volume percent of diluent such as paraffinic oil, which is

* Corresponding author. Address: Department of Rubber Technology, Faculty of Science and Technology, University of Twente, P.O. Box 217, 7500 AE Enschede, The Netherlands. Tel.: +31 53 4892529; fax: +31 53 4893823.

E-mail address: j.w.m.noordermeer@utwente.nl (J.W.M. Noordermeer).

Table 1
Characterization techniques: size ranges [1]

Technique	Resolution
Wide angle X-ray scattering (WAXS)	0.01–1.5 nm
Small angle X-ray scattering (SAXS)	1.5–100 nm
Transmission electron microscopy (TEM)	0.2 nm–0.2 mm
Scanning probe microscopy (STM, AFM...)	0.2 nm–0.2 mm
Scanning electron microscopy (SEM)	4 nm–4 mm
Optical microscopy (OM)	200 nm–200 μ m
Light scattering (LS)	200 nm–200 μ m

often added as a softener and processing aid, obtaining good microscopic images becomes very difficult.

Soft rubber–plastic blends, especially those based on PP as the plastic, are quite common thermoplastic elastomer materials [2]. Compounds of these blends are very popular materials for soft-touch applications such as grips on tools, sports goods, automotive and medical, because the properties of the rubber and the PP phase can be easily tailored into a single product. Understanding the structure–property relationship in these materials is vital for making blends with tailored properties. Studies into these relationships are, however, rather limited, because visualising the blend morphology in these systems has turned out to be rather difficult.

The present paper gives a relative comparison of different microscopic methods that can be used to identify the morphology of highly oil-extended thermoplastic elastomer (TPE) blends based on a soft rubber phase and isotactic polypropylene (PP). TPE blends of two different rubbers with PP were selected for this study. One of them was a dynamically vulcanized blend of ethylene–propylene–diene rubber (EPDM) and PP, and the other one was a blend of styrene–ethylene–butylene–styrene rubber (SEBS) and PP. Dynamic vulcanization implies cross-linking the EPDM phase during the process of melt mixing with PP and the resulting dynamically vulcanized EPDM/PP blends are also referred as thermoplastic vulcanizates (TPVs) [2]. To address the problem of identifying the morphology in case of high loading of rubber along with high loading of oil, all the compositions selected for this study had rubber contents larger than 80 wt% and oil contents higher than 100 wt% with respect to PP. In an attempt to visualise the 3D morphology, electron tomography was carried out on these blends and models of the 3D morphology were constructed. Details of electron tomography principles are given in Refs. [3,4] and its application to polymers including thermoplastic elastomer blends are reported in Refs. [5–7].

2. Experimental

2.1. Materials

The polymers used in the present work were ethylene–propylene–diene terpolymer rubber (Keltan[®] P597; DSM Elastomers B.V.; 63 wt% ethylene, 4.5 wt% 5-ethylidene-2-norbornene (ENB) termonomer), extended with 50 wt% (100 parts per hundred rubber) of paraffinic oil; and a styrene–ethylene–butylene based tri-block copolymer (Kraton[®] G 1651;

Kraton[™] Polymers), with a styrene to rubber ratio of 32:68 wt%. The PP (Stamylan[®] P11E10; Sabic Polypropylenes B.V.) was an extrusion grade with a melt flow index at 230 °C, 2.16 kg of 0.3 g/10 min. The oil used was a paraffinic mineral oil Sunpar[®] 150 containing paraffinic and naphthenic hydrocarbons. For the EPDM formulation a phenolic resin, Schenectady SP[®] 1045 was used as curing agent along with stannous chloride dihydrate (SnCl₂·2H₂O; Merck) as catalyst and zinc oxide (rubber grade; Merck) as acid scavenger. Additionally, stabilizers Irganox[®] 1076 (primary phenolic type antioxidant; Ciba Geigy) and Irgafos[®] 168 (secondary phosphite type antioxidant, Ciba Geigy) were used.

2.2. Melt blending

Ternary blends with a composition of EPDM-or SEBS-rubber/PP/oil were prepared using a Brabender Plasticorder type 350S with a mixer chamber volume of 390 ml and fitted with Banbury type rotors. Mixing was carried out at 180 °C at a rotor speed of 80 rpm. The mixing time was 12 min for TPVs and 20 min for the SEBS/PP/oil blends.

2.3. Compression moulding

After mixing the materials were compression moulded at 200 °C for 3 min under a pressure of 10 MPa and then cooled under pressure to about 30 °C. The moulded sheet thickness was about 2 mm. The sheets were punched into dumbbells (ISO-37, type 2) for tensile measurements.

2.4. Sample preparation and electron microscopy

After compression moulding small samples were taken for electron microscopic examination. Sample preparations for the different microscopic techniques used in this work are described below.

2.4.1. SEM preparations

Samples for SEM were microtomed at –130 °C using a diamond knife mounted on a Leica Ultramicrotome. The samples were then fixed, using a double-sided sticky tape, on a specimen stub. In order to increase the electron density contrast between the rubber and the PP phase, the samples were vapour stained for 30 min using a 1% solution of ruthenium tetroxide. Conductive paints such as carbon suspensions were dabbed onto the tape and base of the specimen to provide contact with the specimen stub. The samples were then coated with a thin layer of gold. The coating was applied in order to provide an electrically conductive layer, to suppress surface charges, to minimize radiation damage and to increase electron emission during SEM. The SEM experiments were performed on a Hitachi S800 scanning electron microscope at an operating voltage of 6 keV.

2.4.2. LVSEM preparations

The LVSEM experiments were done using a Leo 1500 scanning electron microscope at an operating voltage of 1 keV.

The LVSEM was equipped with a secondary electron detector (SE) and a back-scattered electron detector (BSE). The SE detector gives images based on topological contrast while the BSE detector gives images based on phase contrast. Samples to be studied with the SE detector were prepared in two different ways. First, the samples were cryomicrotomed using similar conditions as for conventional SEM. Second, the samples were fractured under liquid nitrogen. Both samples were stained with ruthenium tetroxide vapours for 30 min. For obtaining BSE images the sample must have a flat and smooth surface to completely suppress contributions from the topographic image [1]. So, samples for studying with BSE detector were cryo-microtomed.

2.4.3. TEM preparations

Samples for TEM characterization were prepared by cryomicrotoming 50 nm thin sections at -130°C . The sections were vapour stained using ruthenium tetroxide for 30 min. TEM measurements were performed on a Philips CM 30 transmission electron microscope.

2.4.4. 3D-Tomography

Samples for tomography were prepared by cryomicrotoming to 50 nm thin sections at -130°C . The sections were vapour stained with ruthenium tetroxide for 30 min. Tomography measurements were performed on a Technai 20 TEM. The images were collected digitally with a slow speed CCD camera. A series of 2D TEM images was obtained by tilting the specimen over various tilt angles. The data were corrected for lateral shift and change of defocus, after taking an image. This cycle was repeated, typically, over ± 65 degrees, with 2 degree tilt increments. After the acquisition of a prealigned data set, the data series was aligned more accurately with the help of fiducial markers. Gold beads were previously sprinkled on the TEM grids to aid as markers. After the alignment of the data series the 3D reconstruction was computed using the IMOD image processing and modelling software. The outer surface of the rubber phase was used to build up a contour 3D-model of the rubber phase in each blend [8].

2.4.5. AFM preparations

Samples for AFM were smoothed at -130°C by using a cryomicrotome. The cut surfaces were observed by a

NanoScope III multimode atomic force microscope (Digital Instruments, Santa Barbara, CA, USA) in the tapping mode with phase imaging under ambient conditions. The instrument was equipped with an E-scanner. A standard Si Nanosensor probe was used to conduct the measurements.

3. Results and discussion

3.1. SEM

Conventional SEM-images of a TPV and a SEBS/PP/oil blend are shown in Fig. 1(a) and (b), respectively. The rubber/PP/oil compositions in the images are 28:33:39 wt%.

The oil is distributed on a molecular level between the rubber and amorphous part of PP and, therefore, is not visible in these images. The images show poor contrast between the rubber and PP phases. The picture is blurred and the different features are hardly visible. The image quality even deteriorates with increasing amounts of oil. This problem is caused by sample charging and some beam damage. Charging effects such as bright spots in the image arise due to build up of an electric charge on the specimen surface. Besides, oil being a liquid and an electrical non-conductor, is very unstable under an electron beam. This means that if the accelerating voltage is high, the electrons from the electron beam cannot get to earth. Thus a charge cloud builds up. This suddenly releases its charge during scanning, causing whitening and also darkening of the image. This leads to large contrast differences, which are not controllable during the scan. These problems are common in SEM analysis of biological, hydrated or organic samples and have been well documented [9–11]. Charging can be avoided by working at low acceleration voltages (LVSEM), also known as cross-over voltages, where the number of electrons leaving the surface is just enough to compensate for the incoming ones.

3.2. LVSEM

Low voltage SEM images of a TPV and SEBS/PP/oil blend are shown in Fig. 2(a) and (b), respectively. The rubber/PP/oil composition in this image is 28:33:39 wt%, i.e. the same as in Fig. 1.

The samples were microtomed and stained using ruthenium tetroxide vapours as described in the experimental paragraph.

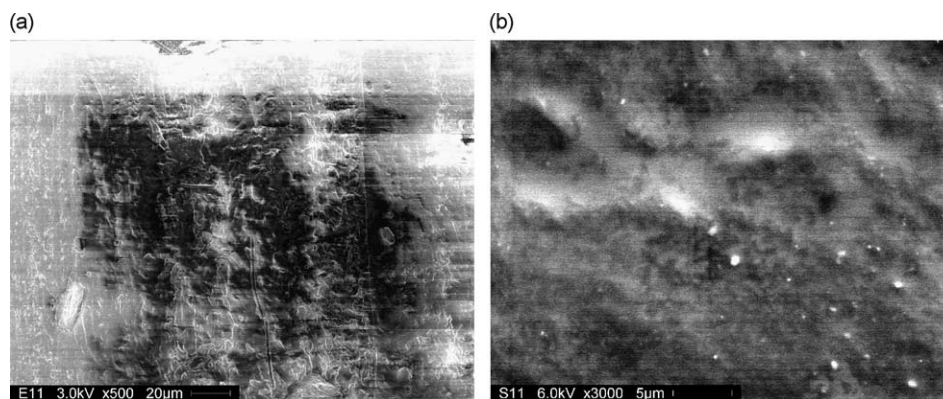


Fig. 1. SEM image of 28:33:39 wt% rubber/PP/oil blend showing poor image contrast between the rubber and PP phase; (a) TPV; (b) SEBS/PP/oil.

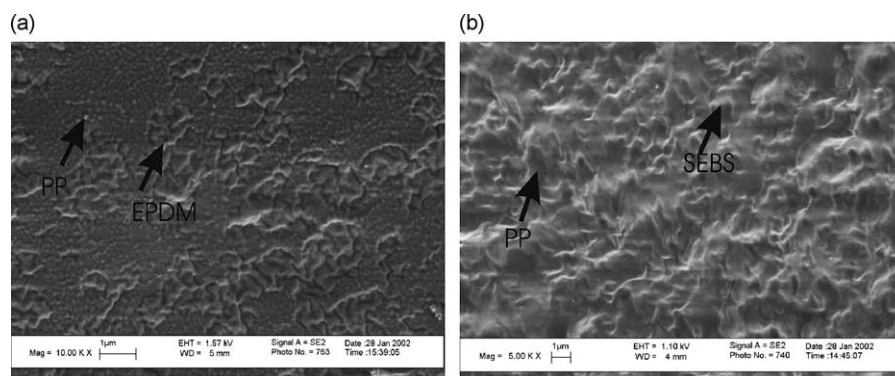


Fig. 2. LVSEM image of 28:33:39 wt% rubber/PP/oil blend showing poor image contrast between the rubber and PP phase; (a) TPV; (b) SEBS/PP/oil.

The micrograph shown in Fig. 2(a) provides a perfect view of the EPDM-phase distributed in PP-matrix. The domains of EPDM appear to be elongated and touching each other. The rubber and the polypropylene phases in the blend were identified after comparison with the SEM-micrographs of the individual components. The charging problem previously seen with conventional SEM is not experienced with this technique. This is because the images were taken at around 1 keV; quite low as compared to the voltages used in conventional SEM. Microtoming of the sample has resulted in a very flat surface in the region of the PP-matrix, while a pronounced relief is observed in the regions of dispersed rubber inclusions. Although the EPDM-domains show a topological contrast different from the PP-matrix and the rubber is preferentially stained with RuO_4 , there is little difference in the grey scales. The small difference in the grey scale levels is most probably due to the similar electron densities of the two phases resulting from poor bulk staining of the sample. If the bulk is relatively poorly stained as compared to the surface, the number of electrons coming out of the rubber- and PP-phases is grossly comparable. The topological contrast is due to a different surface topography of the rubber-phase from the PP-phase at the temperature of observation. The contrast originates from different coefficients of thermal expansion of the rubber- and PP-phases as the material is warmed up from -130°C to room temperature after microtoming [12]. This contrast can be used to best advantage, if the samples are fractured instead of microtomed.

Fractured LVSEM images of TPV and SEBS/PP/oil blends are shown in Fig. 3(a) and (b), respectively. The rubber/PP/oil is 31:25:44 wt%. In Fig. 3(a), the contrast between the EPDM and PP phase is significantly higher, than was observed before. Even the boundaries between EPDM particles are clearly visible. Although the rubber particles overlap each other, they clearly appear to be dispersed in the PP-matrix.

LVSEM reveals many interesting features of the TPV-morphology. The particle size and shape of the EPDM-phase is not uniform. The particle size distribution of EPDM depends on total shear applied to the melt during blending [13]. The particle shape is related to the melt flow index (MFI) of PP. In blends with low MFI, more elliptical particles were reported and as the MFI is increased the particles become more spherical [14].

The SEBS/PP/oil blend, Fig. 3(b), shows a different type of morphology. The SEBS- and PP-phases appear to be co-continuous: it is impossible to distinguish the SEBS phase from the PP-phase. Comparatively more contrast is obtained from LVSEM of extracted blends as shown in Fig. 3(c). The SEBS- and the oil-phases are soluble in toluene at room temperature, leaving the PP-matrix. The amount of SEBS-phase soluble in toluene can be further used to measure the degree of continuity [15]. If all of the SEBS-phase can be extracted, the SEBS-phase must have been continuous. If the PP-phase then remains in one piece and has the same shape as the original sample, the PP-phase must also have been continuous.

In Fig. 3(c), the holes correspond to the removed SEBS-oil phase. The remaining phase is PP. A lot of holes appear to be interconnected along the third dimension, suggesting continuity of the SEBS-phase. Other holes, however, appear to be dispersed. This suggests, that the SEBS-phase is not fully co-continuous. There is a limited degree of connectivity between the SEBS domains, which can be used for quantitative description of the morphology of these blends.

There are several reasons for the enhanced contrast with LVSEM as compared to conventional SEM. The penetration depth of low energy electrons ($< 1\text{ keV}$) is less than 50 nm in organic materials. The image information consequently comes more from regions near to the surface, which are better stained than the bulk. Besides, modern days LVSEM has improved field-emission cathodes in the electron gun that provide narrower probing beams at low as well as high electron energies as compared to conventional SEM. In addition, the in-lens detector in LVSEM gives the possibility to work with a small working distance and, as a consequence with a high resolution at low electrons current. This results in both improved spatial resolution and minimised sample charging and damage.

A comparative study of the secondary electron contrast and back-scattered contrast is given in Fig. 4(a) and (b), respectively. The sample is an EPDM/PP/oil TPV having a composition of 28:33:39 wt%. The resolution of the back-scattered image is lower than the secondary electron image. Back-scattered electrons are emitted from the primary beam and react elastically with the sample's atoms. They are sent back almost in the same direction where they came from, and with very little energy loss [1]. Chemical elements that have

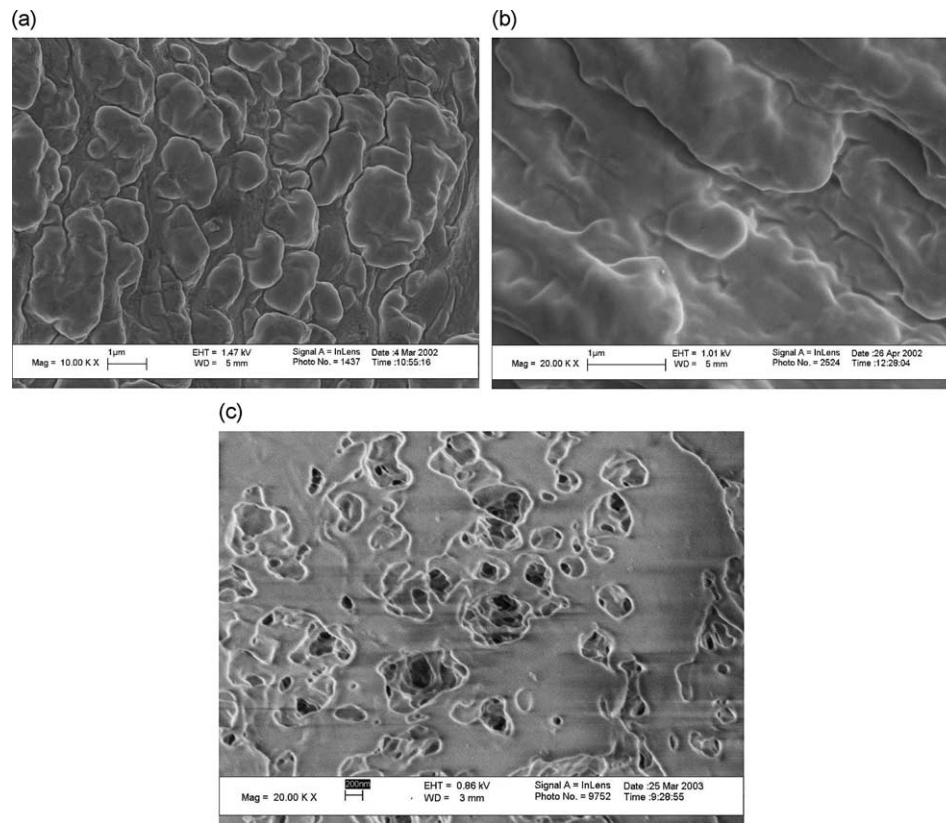


Fig. 3. LVSEM image of 31:25:44 wt% rubber/PP/oil blend. Samples were prepared by cryo-fracture: (a) TPV; (b) SEBS/PP/oil; (c) LVSEM of 31:25:44 wt% SEBS/PP/oil blend after extraction. The image shows the holes left over after the SEBS/oil phase has been extracted.

high atomic number (high positive load of the atomic core) produce more back scattered electrons than the ones that have a low atomic number. The areas of the sample with a high atomic number (here stained EPDM-domains) will thus look whiter

than the ones with a low atomic number. Thus, they give more phase information as compared to secondary electrons. They have higher energy from the secondary electrons and they come from the bulk of the sample. The resolution reached by

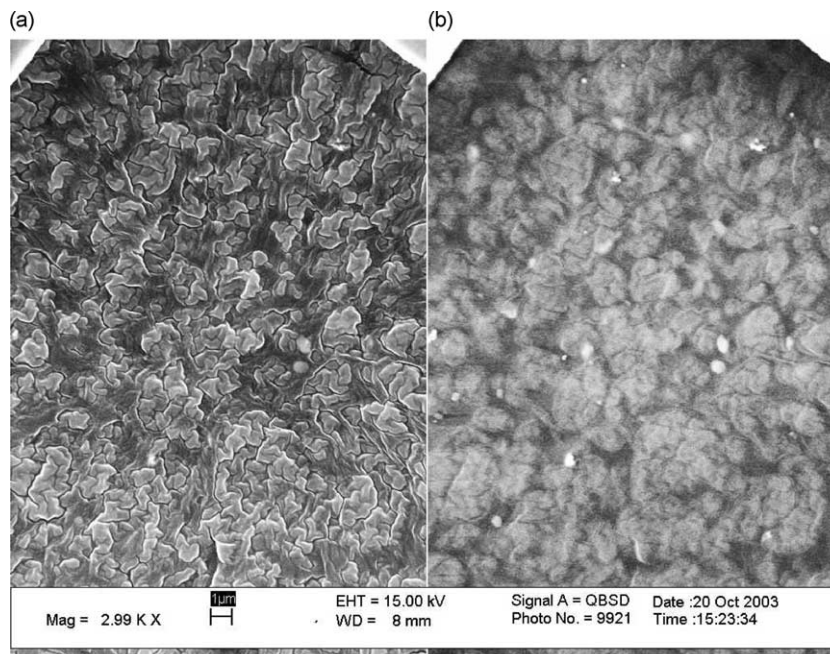


Fig. 4. Comparative LVSEM images of 31:25:44 wt% EPDM/PP/oil TPV obtained using different detectors: (a) secondary electron detector; (b) back scattered electron detector.

back-scattered electrons is quite low. Secondary electrons are emitted when the primary beam, that has lost a part of its own energy, excites atoms of the sample. They are comparatively easier to detect in large numbers with the help of an in-lens detector. So they give images with good signal-to-noise ratio. The image obtained, however, shows the topography of the sample with very little phase contrast. For TPV blends, secondary electron imaging was found to be more useful than back scattered imaging because a high contrast between the phases was necessary to study particle size distribution.

3.3. TEM

TEM-images of TPV and SEBS/PP/oil blends are shown in Fig. 5(a) and (b). The dark phase represents the rubber phase and the white phase is PP. This technique proves to be the best for visualizing the morphology of these blends. The image on the left clearly shows elongated EPDM-domains dispersed in the PP-matrix. The same seems to happen for the SEBS-phase in the image shown on the right. A higher magnification image of the SEBS-phase shows distinct polystyrene domains (Fig. 5(c)) more or less clustered together, and phase separated from the ethylene–butylene matrix. The PP phase is more evenly distributed within the SEBS-phase as compared to the EPDM-phase in Fig. 5(a), which hints in the direction of co-continuous morphology. The contrast between the rubber and the PP-phase is very high as compared to the one seen with LVSEM. The thickness of ultrathin sections (~ 50 nm), staining time (~ 30 min) and the concentration of the staining agent (1% solution of RuO_4) were found to be very crucial for obtaining good images.

The reason why TEM-images could reveal the finest morphological details as compared to LVSEM can be explained by the fact that the image in TEM involves detecting the electrons transmitted through a sample, while SEM involves detecting the number of secondary electrons scattered by the sample. The voltage used in TEM is about 200 keV

while with low voltage SEM it is around 1 keV. This means that the signal to noise ratio is much higher in TEM as compared to LVSEM. The amount of secondary electrons produced in LVSEM is too low to be useful in creating high-resolution images. Detecting transmitted electrons in TEM demands a very thin section: ~ 50 nm. This also reduces sample charging at high acceleration voltages, because the charge on the sample can easily be grounded.

3.4. Electron tomography

Representative tomographic images of co-continuous TPV- and SEBS/PP/oil-blends are shown in Fig. 6(a) and (b), respectively. These images only show the outline of the EPDM-phase in Fig. 6(a) and for the SEBS-phase in Fig. 6(b).

The tomographic images shown in Fig. 6(a) show interesting details of TPV morphology that cannot be observed with conventional TEM. TEM images of TPV samples, having a high loading of EPDM-phase often lead to confusion about the dispersed nature of the EPDM-phase. In those blends, the interparticle distances between the EPDM domains are rather small. Since the image in TEM is a superposition of all EPDM domains present along the electron beam trajectory, in the 2D-image overlapping domains with small interparticle distances appear to touch each other. This gives the impression of a co-continuous EPDM structure. Tilting the sample under TEM during a tomography experiment provides a different side of view, which increases the accuracy of observation and resolves any conflicts about overlapping domains. An example of this effect is given in Fig. 7. The EPDM-domains that appear to touch each other in Fig. 7(a) look separated on tilting, Fig. 7(b). The resulting tomographic model obtained by backprojecting these 2D-TEM images, as shown in Fig. 6(a), conclusively proves the dispersed nature of the EPDM-phase, even in blends containing high amounts of the EPDM-phase.

A TEM image of a 28:33:39 wt% SEBS/PP/oil blend composition was shown in Fig. 5(b). In the image the

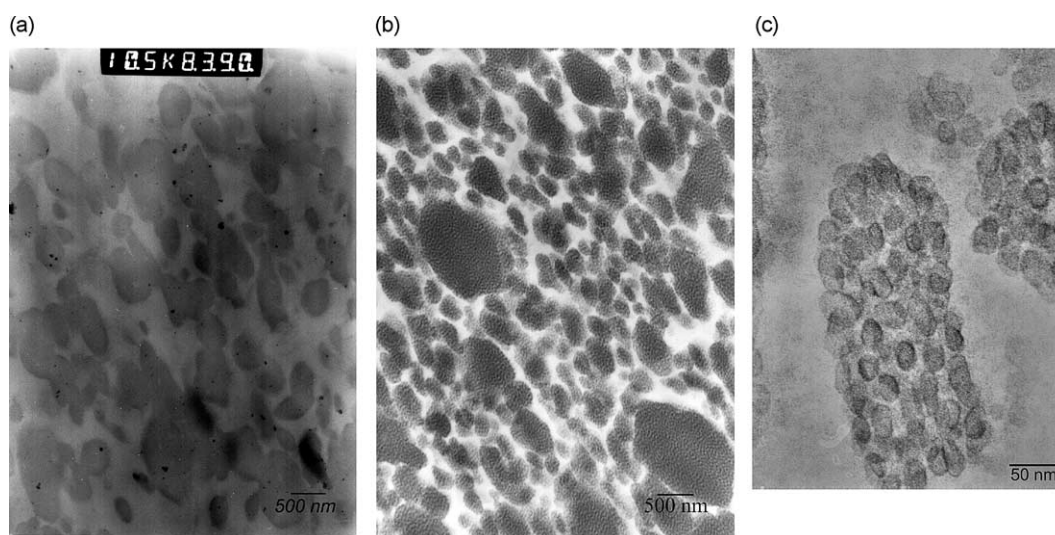


Fig. 5. TEM images of 28:33:39 wt% rubber/PP/oil blend: (a) TPV; (b) SEBS/PP/oil blend; (c) magnified image of the SEBS phase.

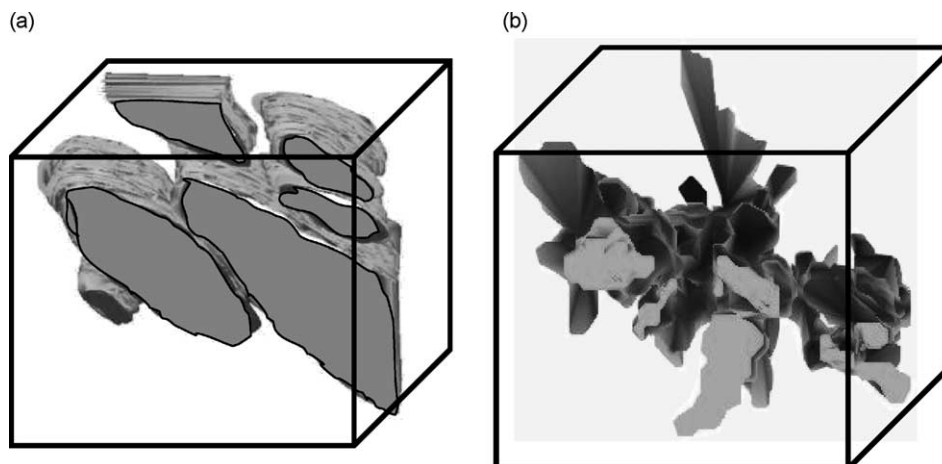


Fig. 6. Tomography images of TPE blends: (a) EPDM/PP/oil TPV; (b) SEBS/PP/oil blend.

SEBS-domains appear black and the PP-phase appears white. It is quite difficult to judge whether the SEBS-domains are dispersed or continuous with the PP phase. The 3D model of this blend obtained using electron tomography is shown in Fig. 6(b). The model shows a SEBS-contour that resembles a complicated double gyroid structure. Although the co-continuous morphology of the SEBS-phase has been studied in the past [15] using confocal scanning laser microscopy, solvent extraction methods, mechanical properties and rheology, the present method gives a direct view of the 3D-structure of these polymer blends at a resolution higher than any of the methods previously reported.

The utility of tomography is twofold: first, it provides a 3D-examination of features, without the need for serial section analysis; second, because the computed slices through the tomographic volumes can be much thinner than is possible to produce by physical sectioning, it reveals structural details in the range of 5–30 nm that tend to be obscured in conventional thin sections [16,17]. In biological sciences, tomographic analysis has forced reassessment of long-standing views of organelles such as mitochondria and Golgi apparatus [16,17]. While biological sciences have a long history of tomographic reconstruction it has rarely been used for materials science. There are several reasons for this:

- Bright field TEM imaging leads to undesirable diffraction contrast from crystalline specimens. By using an imaging technique, which is insensitive to diffraction contrast, such problems may be reduced or eliminated.
- Most material specimens can often be described by 2D TEM projections. This assumption is however not valid for polymer blends especially with high loadings of the rubber phase.
- Until recently, tomography used to be an expensive technique, both in terms of the instruments used and the computational resources required. However, there has been a significant improvement in computing power during the last two years. Softwares and hardwares for reconstruction are both freely available (ex IMOD) and relatively cheap.

All these factors project a bright future towards use of electron tomography in material sciences.

3.5. AFM

AFM images of TPV and SEBS/PP/oil blends are shown in Fig. 8(a) and (b). The rubber/PP/oil composition is 28:33:39 wt%. In these images, the darker grey areas correspond to the rubber phase and the white areas correspond to the PP.

Both images show artefacts due to contamination of the AFM-tip by oil. Such artefacts in the AFM-image were observed earlier in oil-extended blends of s-SBR/BR filled with silica [18,19]. The oil that is present in the compound is squeezed out of the polymer and ends up at the surface, where it is spread out by the AFM-tip. These problems are particularly pronounced at oil contents of more than 100 phr. The image on the left for TPVs shows elongated rubber particles, some of which are completely surrounded by PP matrix, giving the impression that the EPDM-phase is indeed dispersed. The image on the right for the SEBS/PP/oil-blend shows two phases, but it is quite impossible to determine whether the phases are co-continuous. These results indicate that AFM is

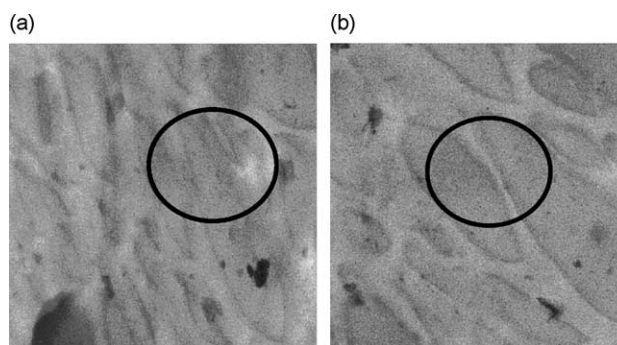


Fig. 7. TEM of EPDM/PP/oil 41:18:41 wt% TPV: (a) no tilt (b) tilted by 45°. The domains of EPDM, which appear to touch each other (as shown by the circle) turn out to be separated in the tilted image.

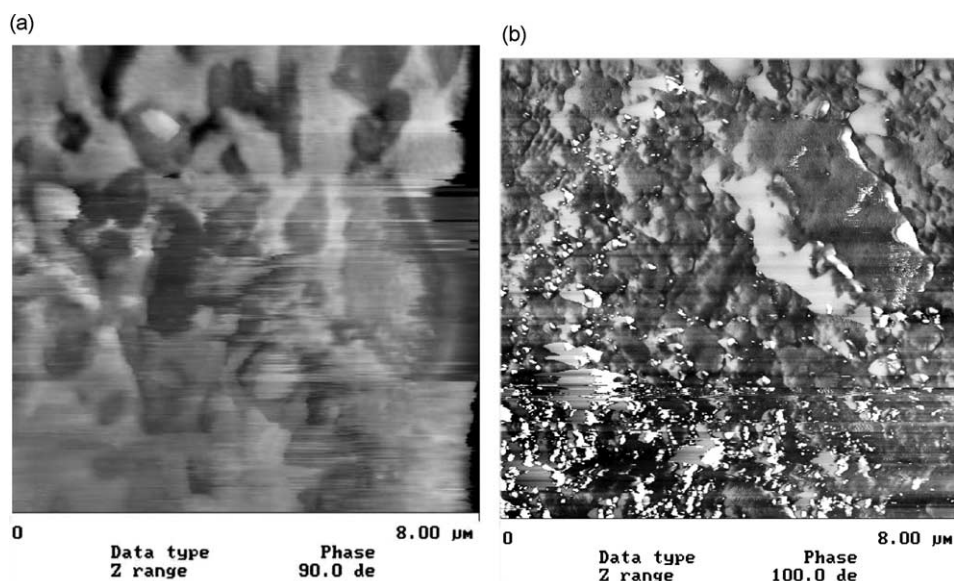


Fig. 8. AFM images of 28:33:39 wt% rubber/PP/oil blend showing poor contrast due to contamination of the AFM tip: (a) TPV; (b) SEBS/PP/oil.

not suitable for investigating the morphology of highly oil-extended soft rubber–plastic TPE blends.

4. Conclusions

The analysis of the morphology of TPV- and SEBS/PP/oil-blends using a variety of techniques leads to the conclusion that TEM is the best method for studying the morphology of these blends. The blend features are clearly resolved and very fine details of the sample can easily be visualised. The small field of view in these images can sometimes be misleading. So, the TEM-micrographs must be supplemented with images obtained from LVSEM. LVSEM of fractured and stained samples gives valuable additional topological information.

Identifying a co-continuous morphology is more difficult than identifying a dispersed phase morphology. For blends with co-continuous morphologies more information is obtained if one of the phases is removed by solvent extraction prior to LVSEM visualization. The degree of co-continuity of the phases can be calculated from solvent extraction data and correlated to microscopic images.

Conventional SEM is not suitable for analysis of soft TPE-blends due to sample charging effects. The reason is most probably the presence of a diluent such as paraffinic oil, which in large amounts builds up a static electric charge on the sample.

AFM, like conventional SEM, works quite nicely with oil free blends, but with samples containing a lot of oil, the tip picks up the oil during scanning, which gives poor images.

Tomography is a valuable tool that gives new 3D-information of objects that cannot be obtained with traditional TEM. The latter gives wrong information due to the fact that the principle of image formation is based on projections. The resolution of TEM is 2–10 times less than one can obtain with tomography. At present, this is the only tool to visualize the 3D morphology of polymer blends.

Acknowledgements

This work was financially supported by Dutch Polymer Institute under project #252. C. Padberg (University of Twente) is acknowledged for performing the AFM measurements and M. Smithers (University of Twente) is acknowledged for performing the SEM, LVSEM and TEM measurements. The authors also acknowledge W. Geerts from University of Utrecht for tomographic measurements.

References

- [1] Sawyer CL, Grubb DT. Polymer microscopy. 2nd ed. London: Chapman and Hall; 1996 [Chapter 1].
- [2] De SK, Bhowmick AK. Thermoplastic elastomers from rubber–plastic blends. New York, NY: Elis Horwood Ltd.; 1990 [Chapter 1].
- [3] Koster J, Ziese U, Verkleij AJ, Janssen AH, Jong KP. *Stud Surf Sci Catal* 2000;130:329.
- [4] Frank J. Electron tomography. New York, NY: Plenum press; 1992.
- [5] Sengupta P, Noordermeer JWM. *Macromol Rapid Commun* 2005;26:542.
- [6] Ziese U, Janssen AH, Murk JL, Geerts WJC, Vander Krift T, Verkleij AJ, et al. *J Microsc* 2002;205:187.
- [7] Crowthers RA, Amos LA, Finch JT, De Rosier DJ, Klug A. *Nature* 1970;226:421.
- [8] Radermacher M. In: Frank J, editor. Weighed back-projection methods in electron tomography. New York, NY: Plenum press; 1992.
- [9] Dudler V, Grob MC, Merian D. *Polym Degrad Stab* 2000;68:373.
- [10] Vezie DL, Adams WW, Thomas EL. *Polymer* 1995;36:1761.
- [11] Butler JH, Joy DC, Bradley GF, Krause SJ. *Polymer* 1995;36:1781.
- [12] Lednický F, Hromádková J, Pientka Z. *Polymer* 2001;42:4329.
- [13] Sengupta P, Noordermeer JWM. *J Elastomers Plast* 2004;36:307.
- [14] Jayraman K, Kolli VG, Kang SY, Kumars S, Ellul MD. *J Appl Polym Sci* 2004;93:113.
- [15] Ohlsson B, Hassander H, Tornell B. *Polym Eng Sci* 1996;36(4):501.
- [16] Perkins G, Frey T. *Micron* 2000;31:97.
- [17] Kremer JR, et al. *J Struct Biol* 1976;116:71.
- [18] Reuvekamp LAEM. Reactive mixing of silica and rubber for tyres and engine mounts—influence of dispersion morphology on dynamic mechanical properties, PhD Thesis, University Twente, The Netherlands; 2003.
- [19] Reuvekamp LAEM, Tenbrinke JW, van Swaaij PJ, Noordermeer JWM. *Kautsch Gummi Kunstst* 2002;55:41.